Characterization of Gene Therapy Associated Uveitis Following Intravitreal Adeno-Associated Virus Injection in Mice

Gayathri Tummala, Adam Crain, Jessica Rowlan, and Kathryn L. Pepple

University of Washington, Department of Ophthalmology, Seattle, Washington, United States

Correspondence: Kathryn L. Pepple, University of Washington, Department of Ophthalmology, Seattle, WA 98104, USA; kpepple@uw.edu.

Received: October 14, 2020
Accepted: January 30, 2021
Published: February 25, 2021

Citation: Tummala G, Crain A, Rowlan J, Pepple KL. Characterization of gene therapy associated uveitis following intravitreal adeno-associated virus injection in mice. *Invest Ophthalmol Vis Sci.* 2021;62(2):41. https://doi.org/10.1167/iovs.62.2.41

Purpose. To characterize the intraocular immune cell infiltrate induced by intravitreal adeno-associated virus (AAV) gene therapy.

Methods. AAV vectors carrying plasmids expressing green fluorescent protein under the control of PR2.1 were injected intravitreally into AAV naive and AAV primed C57Bl/6 mice. Clinical inflammation was assessed using optical coherence tomography. Intraocular immune cell populations were identified and quantified by flow cytometry on days 1, 7, and 29 after intravitreal injection and compared with sham and fellow eye controls.

Results. Optical coherence tomography inflammation score and total CD45+ cell number were significantly higher in AAV injected eyes compared to uninjected fellow eye and sham injected controls. Clinically apparent inflammation (vitritis on optical coherence tomography) and cellular inflammation (CD45+ cell number) was significantly increased in AAV injected eyes and peaked around day 7. Vitritis resolved by day 29, but cellular inflammation persisted through day 29. On day 1, neutrophils and activated monocytes were the dominant cell populations in all AAV injected eyes. On day 7, eyes of AAV exposed animals had significantly more dendritic cells and T cells than eyes of AAV naive animals. By day 29, CD8– T cells were the dominant CD45+ cell population in AAV injected eyes.

Conclusions. Intravitreal AAV injection in mice generates clinically evident inflammation that is mild and seems to resolve spontaneously. However, the total number of intraocular CD45+ cells, particularly T cells, remain elevated. Both innate and adaptive immune cells respond to intravitreal AAV regardless of prior immune status, but the adaptive response is delayed in AAV naive eyes.

Keywords: animal model, uveitis, intravitreal injection, AAV, gene therapy, inflammation, T cell

Adeno-associated virus (AAV) is the most widely used vector platform for gene therapy delivery in many organ systems, including the eye.[1] This is largely due to its wide tissue tropisms, persistent gene expression without genomic integration, and history of safe application. Over thirty ocular gene therapy clinical trials have been performed or are underway for a range of inherited retinal diseases including choroideremia, Leber hereditary optic neuropathy, Stargardt disease, X-linked retinoschisis, and X-linked retinitis pigmentosa.[2] The 2017 FDA approval of Vortigene naeparovec (Luxturna) for the treatment of Leber's congenital amaurosis brought ocular gene therapy into clinical practice, with other clinical trials in phases I/II and III.[3] Apart from the risk of the invasive procedure required to deliver gene therapy to the eye, there is now mounting evidence that uveitis can develop after intravitreal or subretinal vector administration.[4–7] The relevance of gene therapy associated uveitis (GTAU) to therapeutic efficacy and safety, the immune mechanisms responsible, and appropriate treatment strategies to control the inflammation in gene therapy recipients are all important areas of active investigation.

Modeling GTAU in mice provides access to a wide range of genetic and immunologic tools for studying the ocular immune response to gene therapy and for the precise determination of the immune mechanisms involved. Furthermore, this model system provides a good platform for preclinical testing of corticosteroid-sparing strategies that could be used to prevent or manage GTAU in humans. In this study, we establish a reliable murine model of GTAU using an AAV2 capsid and photoreceptor specific green fluorescent protein (GFP) expression cassette. We used this model to characterize the time course and longitudinal cellular populations responsible for GTAU after intravitreal injection. Additionally, we test the impact of prior AAV exposure on GTAU.

Methods

Mice, Vector Preparation, and Intravitreal Injection

Male and female C57BL/6 WT mice ranging in age from 6 to 10 weeks old were bred or purchased from Jackson

Copyright 2021 The Authors

This work is licensed under a Creative Commons Attribution-NonCommercial-NoDerivatives 4.0 International License.

Laboratories (Bar Harbor, ME) and maintained with standard chow and water ad libitum under specific pathogen-free conditions. Drinking water was supplemented with acetaminophen (200–300 mg/kg) after intravitreal injection to minimize discomfort. The animal study protocol was approved by the Animal Care and Use Committee of the University of Washington (animal study protocol #4481-02) and was compliant with ARVO guidelines for use of animals in vision research or by standard laboratory protocols.

Four different AAV preparations (AAV Prep #1–4) were used in the pilot study. Only AAV Prep #2 was used for flow cytometry analysis. The cargo in each preparation is a variation of the PR2.1-RHLOPS construct used by Mancuso et al.[8] AAV Prep #1 cargo was PR2.1-GFPv1.0, which is identical to PR2.1-RHLOPS except that the recombinant human L Opsin (RHLOPS) cDNA was replaced with the coding sequence for eGFP. Prep #1 was packaged into an AAV2 capsid at a titer of 1.45×10^{12} vg/mL. AAV Prep #2 cargo was a modified plasmid called PR2.1-GFPv2.0 (Supplementary Fig. S1B). AAV Prep #2 was packaged into an AAV2 capsid at a titer of 1.5×10^{13} vg/mL. AAV Prep #3 was made using a modified plasmid called PR2.1-GFPv3.0 (Supplementary Fig. S1B), packaged into an AAV2-7m8 capsid[9] at a titer of 4.77×10^{14} vg/mL. AAV Prep #4 was made using a plasmid called PR2.1-GFP SV40 (Supplementary Fig. S1B) packaged into an AAV2-7m8 capsid at a titer of 4.19×10^{14} vg/mL. AAV preps #1, #3, and #4 were packaged using the adenovirus-free triple plasmid method.[9] AAV Prep #2 was packaged by the UW VECTOR core (MDCRC, Muscular Dystrophy Cooperative Research Center) using standard protocols as outlined by Halbert et al.[10] and adapted for AAV2 packaging.

Intravitreal injections were performed as described previously.[11,12] Briefly, animals were anesthetized and topical tetracaine, 2.5% phenylephrine, and 5% betadine were applied to the right eye. We then administered 1.5 µL of viral vector or PBS (sham injection) by intravitreal injection. One month before intravitreal injection, animals in the exposed cohorts received an intramuscular injection of 1.5×10^{13} vg of AAV Prep #2 in 50 µL of 1 M PBS.[13]

Optical Coherence Tomography (OCT) System, Image Acquisition, and Analysis

OCT images were taken as described previously.[12] Briefly, images were acquired using the Bioptigen Envisu R2300 (Bioptigen, Inc., Morrisville, NC). Animals were anesthetized and eyes were dilated with phenylephrine (2.5%, Akorn, Inc., Lake Forest, IL) and corneal protection provided by Genteal (Alcon Laboratories, Inc. Fort Worth, TX). Animals were wrapped in warming gauze and placed in the prone position on the Bioptigen mouse imaging cassette. For the anterior chamber, 3.6 × 3.6 mm images (1000 A-lines/B-Scan × 400 B-scans) were captured using a Bioptigen 12-mm telecentric lens (product # 90-BORE-G3-12; Bioptigen, Inc., Wetzlar, Germany). For posterior chamber imaging, 1.6 × 1.6 mm images (1000 A-lines/B-scan × 200 B-scans) were captured using the Bioptigen mouse retina lens (product # 90-BORE-G3-M; Bioptigen, Inc., Wetzlar, Germany). The degree of clinical inflammation was determined by counting the number of inflammatory cells present in the aqueous or vitreous on an OCT B-scan image. Cell counts were performed by a manual grader masked to eye, treatment, and day. An inflammatory cell was defined as a discrete hyper-reflective dot in the aqueous on anterior segment OCT images or in the vitreous on posterior segment OCT images.

Flow Cytometry

After OCT imaging, the animal was euthanized and both right (injected) and left (fellow, uninjected) eyes were enucleated and intraocular contents collected separately as described by John et al.[14] Briefly, each eye was rinsed in a flow buffer, placed in 50 µL of flow buffer, the cornea and lens removed, and the aqueous humor, iris, vitreous, retina, and retinal pigmented epithelium were collected. The intraocular contents were incubated with 10 mg/mL of DNAse (Roche, Germany) and 0.5 mg/mL of collagenase (Roche, Germany) at 37°C for 25 minutes, and passed through a 70 µg filter and washed with flow buffer. Single cells were counted using a Nexcelom Cellometer Auto 2000 (Nexcelom Bioscience, MA). For each sample, 1×10^6 cells were stained with Zombie Aqua Fixable Viability dye (Biolegend, San Diego, CA) and incubated in Fc Block (2% per sample; Biolegend). The cells were stained with primary antibodies from Biolegend (Lys6G-AF647 [1A8,127609], Lys6C-FITC [HK1.4,128005], CD11b-PerCPCy5.5 [m1/70,101227], CD3-BV421 [17A2, 100228], CD19-BV605 [6D5, 115539], CD11c-APC/fire F780 [N418, 117351], NK1.1-PE [Pk136, 108707], and CD45-BUV395 [30-F11, 565967]) for 30 minutes at 4°C. After staining, cells were washed and fixed with 1% paraformaldehyde in PBS. Data were acquired with a BD LSRII flow cytometer using BD FACSDiva software (BD Bioscience, Franklin Lakes, NJ). Cell counts were obtained using Count-Bright counting beads according to manufacturer protocols. Compensation was performed using single color controls prepared from BD Comp Beads (BD Biosciences). Cell lineages were defined by the following combination of cell surface markers: T cells (CD45+,CD3+,CD19-), B cells (CD45+,CD3-,CD19+), NK cells (CD45+, $CD11b^{lo\text{-}mid}$, NK1.1+), NK T cells (CD45+,$CD11b^{lo\text{-}mid}$, NK1.1+, CD3+), dendritic cells (CD45+, $CD11b^{hi}$,$CD11c^{hi}$), neutrophils (CD45+, $CD11b^{hi}$, Ly6G+), inflammatory macrophages (CD45+,$CD11b^{hi}$, $Lys6C^{hi}$), microglia (CD45+, $CD11b^{hi}$, NK1.1- cd11c-, Ly6c-). The gating strategy is shown in Supplemental Fig. S2. Data analysis was performed using FlowJo v10.1 software (FlowJo LLC, Ashland, OR).

Immunohistochemistry

Eyes were enucleated and fixed in 4% PFA (Electron Microscopy Services, Hatfield, PA) for 1 hour at room temperature (RT), followed by a 30% sucrose solution for 1 hour at RT. OCT Compound (Tissue Tek, Torrance, CA) was added to the 30% sucrose solution to create a 1:1 ratio and eyes were fixed for an additional hour at RT. The eyes were then placed in cryosectioning molds filled with OCT Compound and stored at –80°C. Cryosectioning was performed on the Leica CM 1850. The sections obtained were 8 µm thick. Slides were incubated with PBSTx (Boston Bioproducts, Ashland, MA) for 1 hour at RT, then 5% Normal Goat Serum (Fisher, #01-6201, Hampton, NH) for 1 hour at RT, followed by a 1:200 dilution of GFP antibody (Fisher #A-21311) at +4°C overnight. After 24 hours, the slides were mounted with mounting media + DAPI (Southern BioTech, Birmingham, AL). Images were obtained using an AMG EVOS inverted fluorescence microscope (Advanced Microscope Group, Millcreek, WA).

Investigative Ophthalmology & Visual Science

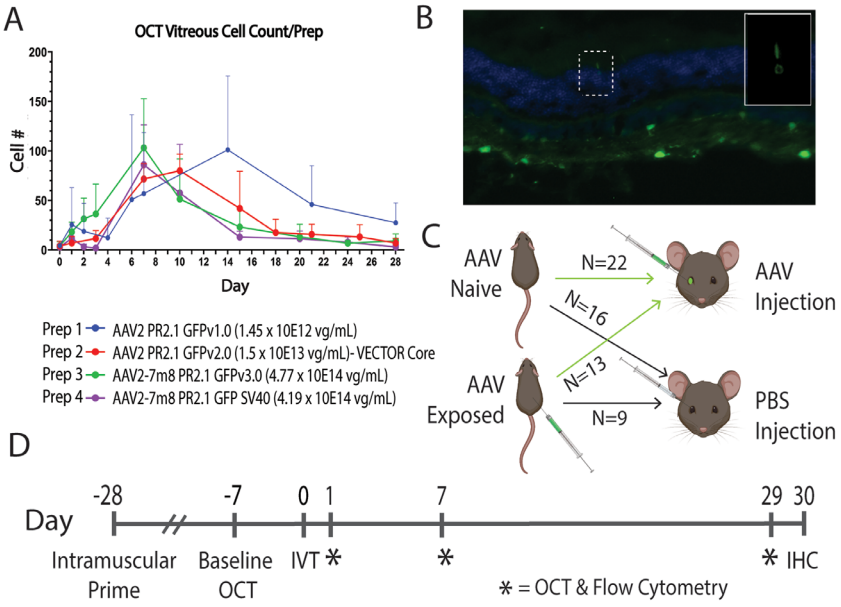

Figure 1. Model illustrating the induction of AAV GTAU. (**A**) Clinical inflammation was scored on OCT images of the posterior segment. Results from four cohorts of mice (AAV Preps #1-4) were combined and the average vitreous cell count per day are shown. (**B**) At 40x magnification, GFP expression (*green*) is detected in a photoreceptor (*white box*) and multiple inner retinal cells 30 days after AAV2-PR2.1-GFP IVT. DAPI (*blue*) marks retinal nuclei. (**C**) Mice that were either naive or exposed to AAV received an intravitreal injection of AAV2-PR2.1-GFP or PBS (sham) in the right eye. (**D**) Outline of experimental study procedures by day. IHC, immunohistochemistry; IVT, intravitreal injection.

Statistical Analysis and Images

Data were graphed and analyzed in GraphPad Prism (version 8.0, GraphPad Software Inc. San Diego, CA). The OCT scores and cell counts were compared between groups on each day using ordinary one-way ANOVA with pairwise post hoc comparisons by Sidak's multiple comparison test. Corrected P values reported with a P value of 0.05 or less were considered significant. Mouse graphics were created with BioRender.com.

Results

There are few reports of visible inflammation in murine eyes after intravitreal injection of AAV gene therapy vectors. We hypothesized that inflammation had been present in prior murine studies, but not detected because it had not been specifically sought. An alternative hypothesis is that inflammation is associated with specific vector variables, including the immunogenicity of specific viral capsids, high viral dose, and contamination from lipopolysaccharide, proteins, or empty viral capsids owing to different packaging protocols.[6,15,16] To address these possibilities, we used serial OCT imaging as a sensitive method for detecting anterior chamber cell and vitritis in murine eyes.[12,17,18] We also tested four different AAV preparations that varied over a range of viral doses (10^9–10^{11} viral genomes/eye), by packaging capsid (AAV2 or AAV2-7m8), cargo plasmid (see maps in Supplementary Fig. S1), or packaging protocol (research laboratory or viral gene therapy core facility) to determine whether the inflammation would be dependent on a variable present in any one preparation.

Eighteen right eyes were injected with one of four AAV preparations (n = 4–5 eyes per preparation) and longitudinal anterior and posterior segment OCT imaging was performed starting the day after intravitreal injection and continued at 2- to 5-day intervals over the course of 1 month. Inflammation on each day was quantified as the total number of vitreous cells identified on the OCT scan centered on the optic nerve head (Fig. 1A, Supplementary Fig. S1A). At baseline, before intravitreal injection, OCT imaging identified vitreous cells in 13 of 18 eyes (mean cell number, 3.7 ± 3.4; maximum cell number, 11). Incident inflammation after intravitreal injection was, therefore, defined as the presence of 10 or more vitreous cells per image and two or more times the baseline number of vitreous cells for the same eye. Anterior chamber (AC) inflammation in the form of AC cells and keratic precipitates was noted sporadically on qualitative analysis. Additional AC quantitative analysis was not performed. On day 1 after intravitreal injection, 10 of the 18 eyes demonstrated incident vitreous inflammation. AAV Prep #1 had an average of 25.5 ± 37.3 cells per image, AAV Prep #2 had an average of 7.0 ± 6.7 cells per image, AAV Prep #3 had an average of 18.2 ± 9.8 cells per image, and AAV Prep #4 had an average of 11.8 ± 5.6 cells per image. On day 7, all AAV injected eyes (18/18) demonstrated incident inflammation. AAV Prep #1 had an average of 57 ± 61.6 cells per image, AAV Prep #2 had an average of 71.8 ± 15.6 cells per image, AAV Prep #3 had an average of 103.2 ± 49.5 cells per image, and AAV Prep #4 had an average of 86.0 ± 40.3 cells per image. By day 28, cell counts had returned to baseline levels in eyes injected with AAV Preps #2, #3, and #4, but remained nonsignificantly elevated in AAV Prep #1 injected eyes (27.5 cells per image ± 20.0; P = 0.40). To verify successful transduction of retinal cells, immunohistochemistry was performed on day 30 eyes. GFP expression was noted in rare photoreceptor cells as well as multiple inner retinal cells (Fig. 1B).

Owing to the development of vitritis detectable by OCT in all injected eyes regardless of AAV preparation variable,

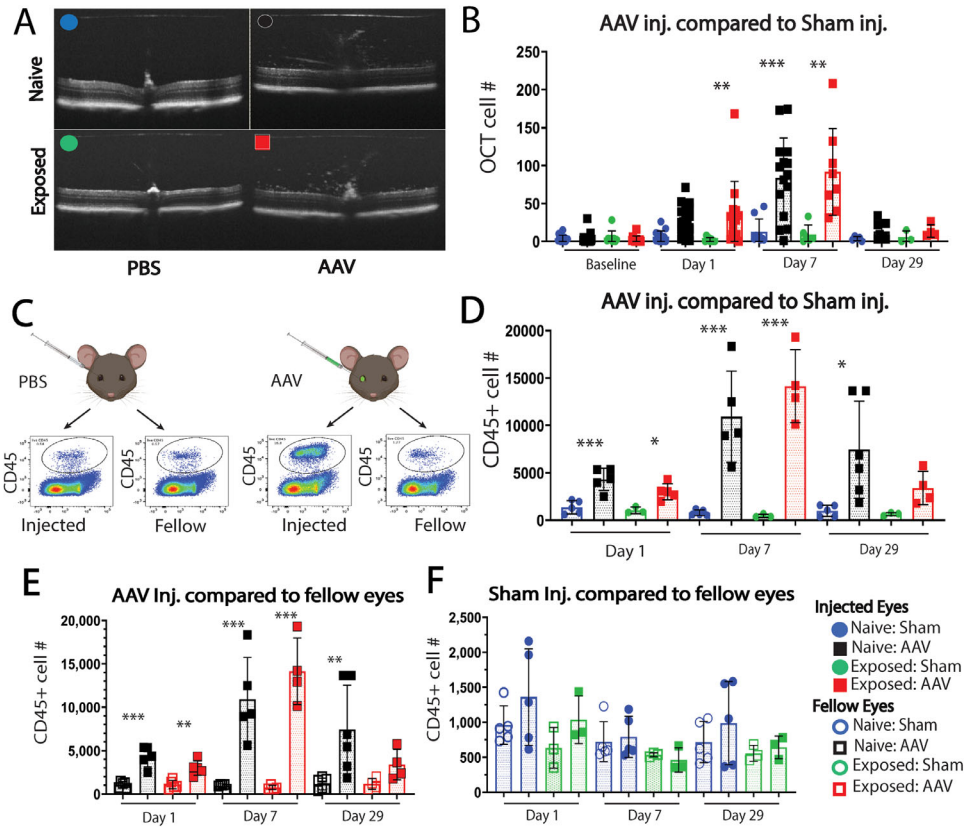

Figure 2. Intravitreal AAV injection generates uveitis in both AAV naive and AAV exposed animals. (**A**) OCT images of the posterior segment of eyes from AAV naive or AAV exposed animals injected with either AAV2-PR2.1-GFP or PBS (sham). Inflammatory cells can be seen in the AAV injected eyes, but not in PBS injected eyes. (**B**) Quantification of inflammatory cells on OCT images obtained at baseline (before injection), day 1, day 7, and day 29 after intravitreal injection. Bars indicate mean and standard deviation. (**C**) Representative day 7 flow cytometry dot plots from injected and fellow eyes illustrating the gate used to quantify intraocular CD45+ cells. (**D**) The total number of CD45+ cells per injected eye for each treatment group on days 1, 7, and 29. (**E**) The total number of CD45+ cells per AAV injected (*right*) eye and uninjected (*left*) fellow eye on days 1,7, and 29. (**F**) The total number of CD45+ cells per sham injected (*right*) eye and uninjected (*left*) fellow eye on days 1, 7, and 29. $^{*}P < 0.05$; $^{**}P < 0.01$; $^{***}P < 0.001$. One-way ANOVA with Sidak's post hoc test.

we concluded that inflammation in murine eyes is likely a common response to intravitreal AAV and that the mouse could be a useful model system for GTAU. To proceed with further mechanistic studies using a vector capsid, preparation protocol, and dose with the best relevance to the vision science community, we selected AAV Prep #2, the AAV2-PR2.1-GFP provided by the gene therapy core facility at 1.5×10^{13} vg/mL (dose 1.5×10^{10} vg/eye).

Next, we designed a study with four treatment arms that would measure the inflammation associated with intravitreal injection of AAV2-PR2.1-GFP and intravitreal injection of PBS (sham) in both AAV naive and AAV exposed animals (Fig. 1C). AAV exposure was provided by intramuscular injection of AAV Prep #2 1 month before intravitreal injection. A total of 25 animals received an intravitreal injection of PBS (Naive:Sham, $n = 16$ or Exposed:Sham, $n = 9$). A total of 35 animals received an intravitreal injection of AAV2-PR2.1-GFP (Naive:AAV, $n = 22$ or Exposed:AAV, $n = 13$). Clinical signs of inflammation were monitored and quantified using OCT imaging. At each time point, a cohort of animals in each treatment arm were sacrificed and eyes were collected for analysis of inflammatory cells by flow cytometry (Fig. 1D). Based on the time course of inflammation determined from the pilot study, day 1 (24 hours after injection) was chosen to evaluate the acute inflammatory response, day 7 was chosen for evaluation of the peak inflammatory response, and day 29 chosen for evaluation of the resolved response.

Baseline OCT imaging was performed on all eyes before intravitreal injection. No significant differences in the baseline vitreous cell number were identified between Sham and AAV injected controls or between the AAV naive or AAV exposed animals (Fig. 2B). On day 1, OCT vitreous cell number increased in AAV injected eyes, but not in sham injected eyes (Naive:Sham 6.4 ± 7.4 cells per image [maximum, 26] vs. Naive:AAV 24.1 ± 20.2 cells per image [maximum 71]; $P = 0.08$) and (Exposed:Sham 2.1 ± 2.8 cells/image [maximum, 8] vs. Exposed:AAV 35.2 ± 44.0 cells/image [maximum, 168]; $P < 0.01$). Day 7 scores in AAV injected eyes were significantly higher than in their respective sham injected control eyes (Naive:Sham 12.8 ± 16.8 cells per image vs. Naive:AAV 83.7 ± 52.7 cells per image [maximum, 174]; $P < 0.001$) and (Exposed:Sham 9.3 ± 12.2 cells per image vs. Exposed:AAV 91.6 ± 57.5 cells per image [maximum, 208]; $P < 0.01$). On day 29, scores in AAV injected eyes had decreased to near baseline levels, and were not increased compared with sham injected controls (Naive:Sham 3.6 ± 2.7 cells per image [maximum, 7] vs. Naive:AAV 13.4 ± 11.7 cells per image [maximum, 34]; $P = 0.08$) and (Exposed:Sham 5.7 ± 8.1 cells per image [maximum, 15] vs. Exposed:AAV 13.8 ± 8.3 cells per image

Investigative Ophthalmology & Visual Science

[maximum, 26]; $P = 0.26$). There were no significant differences in OCT vitreous cell number in Naive:AAV eyes and Exposed:AAV eyes at any time point.

Next, we quantified the number of CD45+ cells present in individual eyes on days 1, 7, and 29 using flow cytometry (Fig. 2C, Supp Fig. S3). Comparisons were made between AAV and sham injected controls (Fig. 2D) and injected eyes and uninjected fellow eyes from the same animal (Figs. 2E, 2F). On day 1, the increase in CD45+ cells in AAV injected eyes was significant when compared with uninjected fellow eyes: Naive:AAV (injected 4305 ± 1174 cells per eye vs. fellow 1083 ± 359 cells per eye; $P < 0.0001$) and Exposed:AAV (injected 2999 ± 849 cells per eye vs. fellow 1094 ± 486 cells per eye; $P < 0.01$) and sham injected controls: (Naive:Sham 1361 ± 689 cells per eye; $P < 0.001$) and (Exposed:Sham 1036 ± 342 cells per eye; $P < 0.05$). The total CD45+ cell number on day 1 was not significantly increased in eyes injected with PBS when compared with uninjected fellow eyes: Naive:Sham (fellow 960 ± 273 cells per eye; $P = 0.48$), and Exposed:Sham (fellow 635 ± 290 cells per eye; $P = 0.67$). CD45+ cell number in AAV injected eyes peaked on day 7 and remained significantly increased when compared with uninjected fellow eyes: Naive:AAV (injected 10,918 ± 4814 cells per eye vs. fellow 941 ± 234 cells per eye; $P < 0.001$) and Exposed:AAV (injected 14,147 ± 3844 cells per eye vs. fellow 745 ± 235 cells per eye; $P < 0.0001$) and sham injected controls (Naive:Sham eyes 791 ± 293 cells per eye; $P < 0.001$) and (Exposed:Sham 461 ± 175 cells per eye; $P < 0.001$). By day 29, the CD45+ cell number decreased from peak levels in Naive:AAV injected eyes, but remained significantly increased when compared with uninjected fellow eyes (Naive:AAV injected 7444 ± 5111 cells per eye vs. Naive:AAV fellow 1152 ± 675 cells per eye; $P < 0.01$) and Naive:Sham injected eyes (987 ± 595 cells per eye; $P < 0.05$). On day 29, the CD45+ cell number decreased from peak levels in Exposed:AAV injected eyes (3392 ± 1758 cells per eye) but remained nonsignificantly elevated when compared with uninjected fellow eyes (1153 ± 619 cells per eye; $P = 0.52$) and Exposed:Sham injected eyes (642 ± 161 cells per eye; $P = 0.68$).

We then compared the impact of prior exposure to AAV on inflammatory cell populations in AAV2-PR2.1-GFP injected eyes over time (Fig. 3). The pie charts depict each cell population as the percent of the total intraocular CD45+ cell population, which represent the average results of four to six individual eyes per time point (Fig. 3A). On day 1 after intravitreal injection, the majority (82%) of CD45+ Cells in Naive:AAV eyes were either neutrophils (42%), Ly6C^{high} macrophages (28%), or retinal microglia (12%). In Exposed:AAV eyes, the same cell types accounted for a slightly smaller majority (71%) with Ly6C^{high} macrophages (35%) comprising the dominant population instead of neutrophils (22%). Exposed:AAV eyes also had a larger proportion of NK cells (7% vs. 2%) and T cells (9% vs. 5%) when compared with Naive:AAV eyes. On day 7, neutrophils had almost completely disappeared from both Naive:AAV and Exposed:AAV eyes (both <2%). In Naive:AAV eyes, Ly6C^{high} monocytes (37%) became the dominant population along with NK cells (22%) and T cells (19%). In contrast, in Exposed:AAV eyes, innate cells such as Ly6C^{high} monocytes (18%) and NK cells (13%) were less populous than T cells (35%). An additional marked difference between the Naive:AAV and Exposed:AAV day 7 results was the greater proportion of dendritic cells in Exposed:AAV eyes (7% vs. <1%). By day 29, T cells were the dominant cell type in both Naive:AAV (49%) and Exposed:AAV (46%) eyes, and all innate cell populations besides retinal microglia had decreased to 10% or less of the total CD45+ cells.

These longitudinal changes in intraocular inflammatory cell populations were also compared using the absolute numbers of each cell type per day (Fig. 3B, Supp Fig. S3). Although there were no significant differences in total CD45+ cell number between AAV injected eyes in either the Naive:AAV or Exposed:AAV animals on any day (Fig. 2D, Fig. 2E), there were significant differences in the total number of certain cell types. On day 1, there were significantly more neutrophils in Naive:AAV eyes (1932 ± 929 cells per eye) than in Exposed:AAV eyes (682 ± 316 cells per eye; $P < 0.001$). On day 7, there were significantly more Ly6C^{high} monocytes in Naive:AAV eyes (3949 ± 1465 cells per eye) than in Exposed:AAV eyes (2615 ± 894; $P < 0.05$). Together, these day 1 and day 7 data suggest a more robust innate immune response in Naive:AAV eyes. In contrast, on day 7, there were significantly more dendritic cells and T cells in Exposed:AAV eyes (DC: 903 ± 195 cells per eye; T cell, 100 ± 2,278 cells per eye) than in Naive:AAV eyes (DC, 46 ± 30 cells per eye [$P < 0.01$]; T cell, 2080 ± 1078 cells per eye [$P < 0.05$]), suggesting an earlier adaptive response in Exposed:AAV animals. However, by day 29, dendritic cell and T cell numbers decreased in Exposed:AAV (DC, 102 ± 82 cells per eye; T cell, 1520 ± 644 cells per eye) and increased in Naive:AAV (DC, 750 ± 670 cells per eye, T cell, 3555 ± 2,438 cells per eye), suggesting the adaptive response was present but delayed in Naive:AAV eyes. On day 29, there were three- to seven-fold fewer T cells and dendritic cells in sham injected eyes than in AAV injected eyes (Naive:Sham: DC, 41 ± 72 cells per eye; T cells, 149 ± 99 cells per eye) and (Exposed:Sham: DC, 5 ± 3 cells per eye; T cell, 232 ± 105 cells per eye), suggesting that the AAV injected eyes were experiencing on-going inflammation. For NK and NK T cells, there were no significant differences in the number of cells in the naive or exposed cohorts, and both conditions demonstrated a similar influx pattern that peaked on day 7 and decreased on day 29.

Owing to the importance of the cytotoxic CD8+ T-cell response in liver toxicity associated with gene therapy for hemophilia,[19] we quantified the number of CD8+ T cells in eyes injected with AAV Prep #2 (Fig. 3B). There were no significant differences in the total number of CD8+ cells between Naive:AAV and Exposed:AAV eyes on any day, but on day 7 there were significantly more CD8– T cells in Exposed:AAV eyes (4069 ± 1986 cells per eye) when compared with Naive:AAV eyes (1358 ± 627 cells per eye; $P < 0.01$), suggesting a more robust CD4+ T-cell response in the AAV exposed condition.

Discussion

In this study, we demonstrate the consistent induction of GTAU in mice after intravitreal injection of an AAV2 gene therapy vector. GTAU manifested clinically as vitritis that was detectable both by OCT imaging and by significant increases in intraocular CD45+ cells. Importantly, although the clinically apparent vitritis subsided after 1 month, the increase in total intraocular CD45+ cells persisted, and were predominantly T cells regardless of prior AAV exposure. To our knowledge, this study is the first to investigate GTAU inflammatory cell infiltrate in ocular tissues longitudinally and with flow cytometry. Despite the downregulatory immune environment in the eye, we show that all the major cell types of

Investigative Ophthalmology & Visual Science

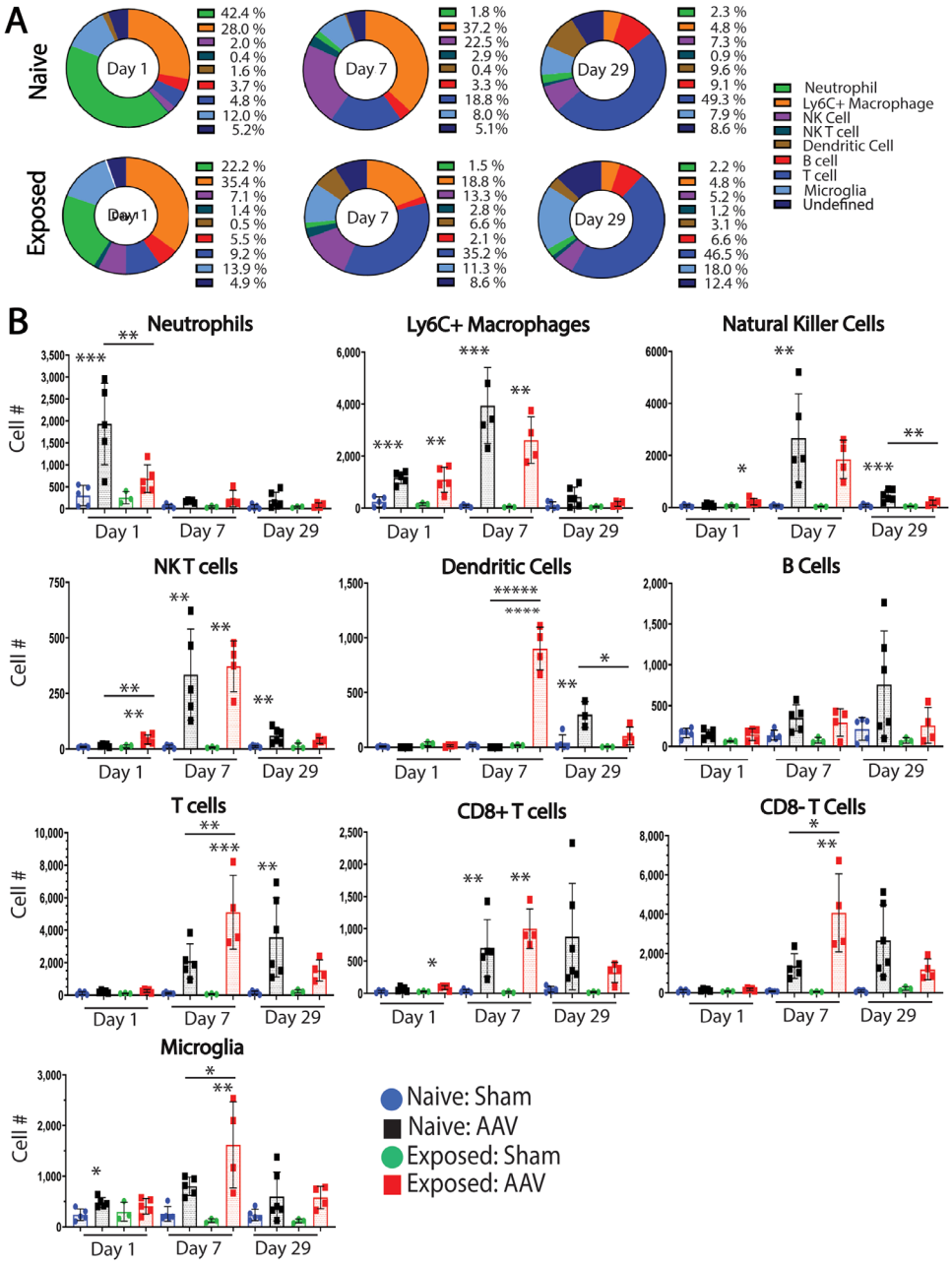

Figure 3. Prior AAV exposure impacts leukocyte population dynamics over the time course of GTAU. (**A**) Pie graphs showing intraocular inflammatory cell populations in Naive:AAV and Exposed:AAV injected eyes as a percent of the total $CD45^{+}$ cells on day 1, day 7, and day 29 after IVT of AAV2-PR2.1-GFP. (**B**) Graphs of total cell number in AAV and sham injected eyes for each treatment group by cell type and by day. Comparisons of results for each cell type across all days were performed with a one-way ANOVA test. For significant results ($P < 0.05$), post hoc pairwise comparisons between Naive:AAV and Exposed:AAV by day were performed using Sidak's test. Adjusted P values indicated by * for $P < 0.05$, ** for $P < 0.01$, and *** for $P < 0.001$. IVT: intravitreal injection.

the innate and adaptive immune response respond to this intervention. Our work also provides an initial timeline for when the various cell types enter and leave the eye. The antigen specificity of the T cells and whether or not they are proinflammatory or possibly regulatory remains to be determined, but their presence raises the possibility that the uveal tissues of the eye experience ongoing cellular inflammation after intravitreal gene therapy that is not readily apparent on clinical examination.

In this model of GTAU, the intensity and timing of the uveitis were not impacted by prior exposure to AAV2. In both the exposed and naive conditions, low-level inflammation was noted in AAV injected eyes on day 1 and increased significantly, peaking on day 7. The inflammation regressed spontaneously over the next month. The inflammatory infiltrate demonstrated an early innate response that was replaced by a T-cell–dominant adaptive response regardless of prior exposure status. However, there were significant differences in the day when specific immune cell types arrived in the eye based on prior AAV exposure. In general, Naive:AAV eyes demonstrated a stronger innate immune response than Exposed:AAV eyes on days

Investigative Ophthalmology & Visual Science

1 and 7 (neutrophils, macrophages, and NK cells). These findings may be explained by the presence of neutralizing antibodies in the vitreous of Exposed:AAV eyes that could have impacted vector concentration and decreased early innate signaling within the eye.[15,20] Priming also influenced the timing of the adaptive immune response. Both dendritic cells and T cells were significantly more numerous in Exposed:AAV eyes than in Naive:AAV eyes on day 7. This result reversed on day 29 when dendritic cells and T cells were more numerous in Naive:AAV eyes, suggesting that the adaptive immune response in this group was delayed but not absent.

In our pilot study, incident inflammation was generated by two capsid variants, intravitreal doses ranging from 10^9 to 10^{11} vg/eye, cassettes with differing introns, and vector produced both by our laboratory and a viral gene therapy core facility. We concluded from these results that GTAU is common and represents an immune response to intravitreal AAV and/or its cargo. However, we did not specifically control for the possibility that inflammation could be the result of a common contaminant or owing to different contaminants with varied immunogenic potential produced by the independent packaging protocols. Additionally, alternative promoters, cargo genes, and clinically important serotypes such as AAV8, AAV2/5, AAV2/8, and AAV2tYF were not tested. Further testing of these variables will help to determine to what extent our findings are generalizable.

Despite the general safety and efficacy that has been observed in a large number of preclinical and human studies, there is a growing appreciation for the possibility of inflammation following intravitreal and subretinal AAV gene therapy.[4–7] The field now needs to balance the benefits of gene therapy treatments on vision recovery with the risks of inflammation and subsequent corticosteroid treatment. Multiple factors appear to contribute to GTAU in humans, including the total viral genome dose, route and method of vector administration, vector preparation, purity, and empty capsid burden.[21] Until recently, reports of GTAU in preclinical models were limited, and few studies have systematically tested the impact of changing individual variables on the risk of GTAU.[15,16,22] When choosing which models are best suited to test these variables, it is important to closely consider the model's ability to mimic the human immune response, the availability of reagents, and financial and ethical considerations. It is unlikely that a single model system will prove superior for all considerations. Several components of this murine model make it highly desirable for use in studying GTAU. Importantly, the time course and intensity of the inflammatory response mirrors the reports of inflammation from human clinical trials.[6] In addition, the genetic and molecular tools available in a murine system allow for rapid, broad-based, and well-controlled hypotheses testing that is not available in most other model organisms. However, we acknowledge that there are limitations to the murine model system as a model for human eye disease and recognize the need for studies utilizing larger animal and nonhuman primate (NHP) models. As part of a coordinated approach, studies with mice should be included to help narrow the range of mechanistic hypotheses to a small number of high-yield hypotheses appropriate for testing in larger animal and NHP models.

Similar to the results in our study, previous work by Reichel et al.[23] in NHPs identified evidence of a robust adaptive immune response developing 7 days after the injection of rAAV8.hCNGA3 in animals with baseline AAV8 seropositivity. In this NHP study, the authors identified increasing serum titers of anti-AAV8 antibodies in animals receiving intravitreal and high-dose subretinal injections. Although we did not measure the humoral response in mice, our results did identify both T and B cells within AAV2 injected eyes starting on day 7. These similarities in the timing of the adaptive response suggest that the murine and NHP model systems share relevant features after exposure to intravitreal AAV.

It is important to keep in mind that the majority of retinal gene therapy clinical trials use a subretinal approach for vector delivery instead of an intravitreal approach. However, during subretinal injection, reflux from the subretinal bleb into the vitreous humor can occur and may be a factor contributing to the development of vitritis in some eyes.[24,25] A vitrectomy is performed before subretinal injection in human and NHP studies and this step cannot be replicated in the mouse model; however, understanding the immune response to AAV therapies that escape the subretinal space will help to clarify the importance of this variable on patient outcomes. Among the clinical trials utilizing an intravitreal approach, the ongoing X-linked retinoschisis trial (NCT02317887) found dose-related inflammation in multiple subjects as well as a dose-related increase in serum AAV8 antibodies.[26] Additionally, the subject in this trial who developed the most significant GTAU with 3+ AC cell, 2+ vitreous cell and haze, and retinal vasculitis also developed a postinflammatory posterior vitreous detachment complicated by retinal tear and subsequent vitreous hemorrhage. Although this experience has not been the case for the majority of ocular gene therapy patients, it does highlight the need to understand and control the ocular immune response in future trials.

Another consideration is the impact of prior retinal degeneration on the timing and character of the immune response to gene therapy. Microglia are important mediators of neuroinflammation and play a role in retinal degeneration.[27–29] In this study, we determined the cellular response in wild-type nonretinal degenerate eyes. Using disease-specific mice that model specific forms of retinal degeneration in humans will help to predict how preexisting retinal disease will impact the immune response to gene therapy. A final, clinically relevant question is the efficacy of a subsequent intravitreal injection in the contralateral eye. Li et al.[30] reported decreased transduction efficacy of a subsequent contralateral intravitreal injection attributed to the presence of neutralizing antibodies. Our data suggest the possibility that a CD8+ T-cell response is also generated by intravitreal injection, which will need to be confirmed with antigen-specific testing. For contralateral eye injections using the intravitreal route, this raises the additional concern that a cytotoxic T-cell response could remove cells that were successfully transduced.

The limitations of this study include not exploring the immune response to subretinal gene therapy delivery. One group has demonstrated retinal and RPE toxicity after subretinal injection of vectors with promoters that induced ubiquitous RPE expression, but no toxicity with photoreceptor specific promoters.[16,31] It is currently unknown if the same mechanisms driving GTAU after intravitreal injection are also responsible for the toxic effects seen after subretinal injection. This study also did not address the question of antigen specificity of the adaptive immune response or the possibility that innate immune function is sufficient for GTAU. Rather, this study identifies the

Investigative Ophthalmology & Visual Science

feasibility of using this model to begin to answer these important questions. Future studies should therefore explore the antigen specificity of the adaptive immune response, recurrent inflammation beyond 30 days, the efficacy of a second contralateral injection, the mechanistic underpinnings of GTAU beginning with the role of the innate immune response, and the impact of subretinal injection of AAV2-PR2.1-GFP.

In summary, intravitreal injection of AAV2-PR2.1-GFP in mice consistently generates clinically evident inflammation that is mild and seems to resolve spontaneously in a manner similar to reports of inflammation in human clinical trials. Importantly, although most eyes showed spontaneous clinical improvement, signs of cellular inflammation persisted and were of unclear clinical significance. The murine model presented here will be useful for studying the mechanisms of GTAU and provide valuable insights that may inform future therapies in humans.

Acknowledgments

The authors thank Maureen Neitz for support on this project including providing AAV Prep #1, technical support, and review of the manuscript, as well as Richard Moore for assistance with the immunohistochemistry portion of this project.

Supported by funding from a Research to Prevent Blindness career development award, the Alcon Research Institute Young Investigators Grant, K08 EY023998, R01EY030431, P30-001730 Core Grant, an unrestricted grant from Research to Prevent Blindness, and support from the Mark J. Daily, MD Research Fund and the Graham and Brenda Siddall Uveitis Research Fund.

Disclosure: **G. Tummala,** None; **A. Crain,** None; **J. Rowlan,** None; **K.L. Pepple,** None

References

1. Wang D, Tai PWL, Gao G. Adeno-associated virus vector as a platform for gene therapy delivery. *Nat Rev Drug Discov*. 2019;18:358–378.
2. Rodrigues GA, Shalaev, E, Karami, TK, Cunningham, J, Slater, NKH, Rivers, HM. Pharmaceutical development of AAV-based gene therapy products for the eye. *Pharm Res*. 2018;36:29.
3. Moore NA, Morral N, Ciulla TA, Bracha P. Gene therapy for inherited retinal and optic nerve degenerations. *Expert Opin Biol Ther*. 2018;18:37–49.
4. Bainbridge JWB, Smith, AJ, Barker, SS, et al. Effect of gene therapy on visual function in Leber's congenital amaurosis. *N Engl J Med*. 2008;358:2231–2239.
5. Bainbridge JWB, Mehat, MS, Sundaram, V, et al. Long-term effect of gene therapy on Leber's congenital amaurosis. *N Engl J Med*. 2015;372:1887–1897.
6. Bouquet C, Clermont, CV, Galy, A, et al. Immune response and intraocular inflammation in patients with Leber hereditary optic neuropathy treated with intravitreal injection of recombinant adeno-associated virus 2 carrying the ND4 gene: a secondary analysis of a phase 1/2 clinical trial. *JAMA Ophthalmol.* 2019;137:399–406.
7. Dimopoulos IS, Hoang, SC, Radziwon, A, et al. Two-year results after AAV2-mediated gene therapy for choroideremia: the Alberta Experience. *Am J Ophthalmol*. 2018;193:130–142.
8. Mancuso K, Hauswirth, WW, Li, Q, et al. Gene therapy for red-green colour blindness in adult primates. *Nature*. 2009;461:784–787.
9. Flannery JG, Visel M. Adeno-associated viral vectors for gene therapy of inherited retinal degenerations. *Methods Mol Biol*. 2013;935:351–369.
10. Halbert CL, Allen JM, Chamberlain JS. AAV6 vector production and purification for muscle gene therapy. *Methods Mol Biol*. 2018;1687:257–266.
11. Choi WJ, Pepple KL, Zhi Z, Wang RK. Optical coherence tomography based microangiography for quantitative monitoring of structural and vascular changes in a rat model of acute uveitis in vivo: a preliminary study. *J Biomed Opt*. 2015;20:016015.
12. Gutowski MB, Wilson L, Van Gelder RN, Pepple KL. In vivo bioluminescence imaging for longitudinal monitoring of inflammation in animal models of uveitis. *Invest Ophthalmol Vis Sci*. 2017;58:1521–1528.
13. Li H, Lin, SW, Giles-Davis, W, et al. A preclinical animal model to assess the effect of pre-existing immunity on AAV-mediated gene transfer. *Mol Ther*. 2009;17:1215–1224.
14. John S, Rolnick, K, Wilson, L, et al. Bioluminescence for in vivo detection of cell-type-specific inflammation in a mouse model of uveitis. *Sci Rep*. 2020;10:11377.
15. Timmers AM, Newmark, JA, Turunen, HT, et al. Ocular inflammatory response to intravitreal injection of adeno-associated virus vector: relative contribution of genome and capsid. *Hum Gene Ther*. 2020;31:80–89.
16. Xiong W, Wu, DM, Xue, Y, et al. AAV cis-regulatory sequences are correlated with ocular toxicity. *Proc Natl Acad Sci USA*. 2019;116:5785–5794.
17. Chu CJ, Gardner, PJ, Copland, DA, et al. Multimodal analysis of ocular inflammation using the endotoxin-induced uveitis mouse model. *Dis Model Mech*. 2016;9:473–481.
18. Jiao H, Hill LJ, Downie LE, Chinnery HR. Anterior segment optical coherence tomography: its application in clinical practice and experimental models of disease. *Clin Exp Optom*. 2019;102:208–217.
19. Kumar SRP, Hoffman BE, Terhorst C, de Jong YP, Herzog RW. The balance between CD8+ T cell-mediated clearance of AAV-encoded antigen in the liver and tolerance is dependent on the vector dose. *Mol Ther*. 2017;25:880–891.
20. Li Q, Miller R, Han PY, et al. Intraocular route of AAV vector administration defines immune response and therapeutic potential. *Invest Ophthalmol Vis Sci*. 2008;49:4759–4759.
21. Verdera HC, Kuranda K, Mingozzi F. AAV vector immunogenicity in humans: a long journey to successful gene transfer. *Mol Ther*. 2020;28:723–746.
22. Reichel FF, Dauletbekov, DL, Klein, R, et al. AAV8 can induce innate and adaptive immune response in the primate eye. *Mol Ther*. 2017;25:2648–2660.
23. Reichel FF, Peters, T, Wilhelm, B, et al. Humoral immune response after intravitreal but not after subretinal AAV8 in primates and patients. *Invest Ophthalmol Vis Sci*. 2018;59:1910–1915.
24. Xue K, Groppe M, Salvetti AP, MacLaren RE. Technique of retinal gene therapy: delivery of viral vector into the subretinal space. *Eye*. 2017;31:1308–1316.
25. Vasconcelos HM, Jr., Lujan BJ, Pennesi ME, Yang P, Lauer AK. Intraoperative optical coherence tomographic findings in patients undergoing subretinal gene therapy surgery. *Int J Retina Vitreous*. 2020;6:13.
26. Cukras C, Wiley, HE, Jeffrey, BG, et al. Retinal AAV8-RS1 gene therapy for X-linked retinoschisis: initial findings from a phase I/IIa trial by intravitreal delivery. *Mol Ther*. 2018;26:2282–2294.
27. Zhao L, Zabel, MK, Wang, X, et al. Microglial phagocytosis of living photoreceptors contributes to inherited retinal degeneration. *EMBO Mol Med*. 2015;7:1179–1197.

28. Yu C, Roubeix C, Sennlaub F, Saban DR. Microglia versus monocytes: distinct roles in degenerative diseases of the retina. *Trends Neurosci*. 2020;43:433–449.
29. Rashid K, Akhtar-Schaefer I, Langmann T. Microglia in retinal degeneration. *Front Immunol*. 2019;10: 1975.
30. Li Q, Miller, R, Han, PY, et al. Intraocular route of AAV2 vector administration defines humoral immune response and therapeutic potential. *Mol Vis*. 2008;14:1760.
31. Ye G-J, Budzynski, E, Sonnentag, P, et al. Cone-specific promoters for gene therapy of achromatopsia and other retinal diseases. *Hum Gene Ther*. 2016;27:72–82.